Journal of Applied Science and Agriculture, 10(5) Special 2015, Pages: 149-158

AENSI Journals

JOURNAL OF APPLIED SCIENCE AND AGRICULTURE

ISSN 1816-9112

Journal home page: www.aensiweb.com/JASA

Microstructural Characterizations and Mechanical Properties in Friction Stir Welding Technique of Dissimilar (Al-Cu) Sheets

[1,2]H.I. Dawood, [1]Kahtan S. Mohammed, [1]Azmi Rahmat, [3]M.B. Uday

[1]Universiti Malaysia Perlis, School of Materials Engineering, Taman Muhibah-Jejawi-Arau 02600 Perlis, Malaysia.
[2]Department of Chemical Engineering, College of Engineering, University of AL-Qadisiya, 88 Qadisiya, Iraq.
[3]UTM - Centre for Low Carbon Transport in cooperation with Imperial College London, Transportation Research Alliance, Universiti Teknologi Malaysia 81310 Skudai, Johor, Malaysia.

A R T I C L E I N F O

Article history:
Received 31 December 2014
Received in revised form 26 January 2015
Accepted 28 January 2015
Available online 11 February 2015

Keywords:
Friction stir welding, dissimilar joints, heat affected zone, nugget zone, rotational speed, intermetallic compounds.

A B S T R A C T

In this study, dissimilar sheets of commercially available pure aluminium and copper, were butt joined by friction stir welding (FSW) with a thickness of 3mm to explore the effect of tool rotational speeds on microstructures and mechanical properties experimentally. Three rotational speeds of 1000, 1750 and 2000 rpm were applied. The transverse speed and the axial force were kept constant at 30 mm/min and 7.5 KN, respectively. The cylindrical shoulder and conical pin tool was used to produce the joints. Macrostructures, microstructures, X-ray diffraction (XRD), Vickers microhardness and tensile strength were investigated at these different rotational speeds. The joint welded at 1750 rpm was compared with their counterparts and observed significantly better. The formation of relatively hard brittle intermetallic compounds (Al2Cu and Al4Cu9) were observed with the joint fabricated at rotational speed of 2000 rpm. The results of microhardness (HV) at the nugget zone (NZ) were superior to those of thermomechanically affected zone (TMAZ), heat affected zones (HAZ) and the base metal (BM). At the rotational speed of 1750 rpm, the tensile strength was higher than other joints. The examination of fractural surface showed that when the dissimilar joints were affected with increasing rotational speeds or heat input; the fracture mode had a tendency to change from ductile to brittle mode.

© 2015 AENSI Publisher All rights reserved.

To Cite This Article: H.I. Dawood, Kahtan S. Mohammed, Azmi Rahmat, M.B. Uday., Microstructural Characterizations and Mechanical Properties in Friction Stir Welding Technique of Dissimilar (Al-Cu) Sheets. ***J. Appl. Sci. & Agric.,*** *10(5): 149-158, 2015*

INTRODUCTION

As a newly-developed solid-state joining technique, FSW has many advantages including low processing temperature, easy work-piece preparation and microstructural refinement. FSW is a clean, environmental friendly and non-harmful process as it is not accompanied by an arc formation, radiation and toxic gas emission (Shukla & Shah, 2010). Nowadays, FSW technique has a wide potential application in aerospace, ship building, automobile and in other manufacturing industries. It has been applied widely to join metallic materials such as aluminium, magnesium and copper alloys (Mishra & Ma, 2005; Nandan, DebRoy, & Bhadeshia, 2008). A high-quality joint of dissimilar aluminium and copper is hard to be produced by fusion welding techniques due to the large differences between melting points and thermal conductivities (Ouyang, Yarrapareddy, & Kovacevic, 2006; Weigl, Albert, & Schmidt, 2011). Therefore, dissimilar welding of aluminium and copper is a challenging technique to be developed, and welding of these two metals is a key problem to be solved. Several problems (Joint defects) have been found when using conventional fusion welding technologies, such as voids and inclusions can seriously compromise the mechanical performance of the welding joint. Moreover, gas protection shields have to be used which add another complexity to the whole process (Vural, Ogur, Cam, & Ozarpa, 2007).

Investigating the joint properties of aluminium 6061 alloy and copper by FSW was performed and considered difficult to weld due to major differences between their hardnesses, melting points, electric and thermal conductivities. However, the generated heat required is much higher than in almost any other materials(Shukla & Shah, 2010). (Kwon, Shim, & Park, 2009), have studied the effect of tool rotational speeds (500 rpm, 1000 rpm, 2000 rpm and 3000 rpm) on the microstructures and mechanical properties of aluminium alloys using FSW technique. They

Corresponding Author: H.I. Dawood, Universiti Malaysia Perlis, School of Materials Engineering, Taman Muhibah-Jejawi-Arau 02600 Perlis, Malaysia.

observed that high rotational speeds could raise rate of strain and thereby affect the recrystallization process. In general, the size of dynamically recrystallized grains in the NZ decreases with the increase of the strain rate. A higher tool rotational speed also results in a higher temperature and slows the cooling rate. On the other hand, a lower heat input condition due to a lower rotational speed results in lack of stirring action and causes formation of defects (Elangovan & Balasubramanian, 2007). (Galvao, Oliveira, Loureiro, & Rodrigues, 2011), studied the effect of process parameters on the formation and distribution of brittle structures using aluminium and copper. They observed when increasing heat input, the dimension of mixed material zones and homogeneity were also increased. In FSW of dissimilar metals, one of the concerns is the formation of brittle intermetallic compounds such as Al2Cu, AlCu and Al4Cu9 which are responsible for preferential development of cracks in the tensile test (Shukla & Shah, 2010). (P. Liu, Shi, Wang, Wang, & Zhang, 2008), observed that there were no new Al-Cu intermetallic compounds in the welding of Copper (T2) and aluminium alloy (5A06). (Mishra & Ma, 2005) pointed out that FSW of dissimilar metals of aluminium and copper was not successful in sound joint production. Until present, the available studies on dissimilar FSW of aluminium and copper has little interest. There are many problems to be solved including deep understanding of the microstructure evolution and optimization of processing parameters. However, according to our knowledge no studies have so far evaluated dissimilar joining of commercially available pure aluminium and copper metals, because of the great difference in hardness between pure Al and Cu. Therefore, welding of Al alloys (instead of pure Al) with Cu has been researched. The aim of this study was to investigate the effect of tool rotational speeds on the macrostructure, microstructure, XRD, Vickers microhardness, tensile strength and fractural surface of the tensile test of dissimilar commercially available pure aluminium and copper joints produced by FSW.

1. Methodology:

1.1 Materials and FSW Process:

FSW of regular butt joint configuration on dissimilar commercially available pure aluminium and copper sheets was investigated, with a thickness of 3mm supplied by Heap Sing Metal and Machinery (Sdn. Bhd, Malaysia). The workpieces were cut into the size of (100×75 mm) using a cutting band saw machine (MODEL: UE-712A). The chemical compositions of the base materials are listed in Tables 1 and 2. In FSW, the advancing side (AS) is the side where the velocity vector of the rotational tool and transverse speed are in the same direction; whereas the side where the velocity vector are opposite is referred to the retreating side (RS). Copper, which is a harder material, was placed on the AS; while aluminium sheets were clamped on RS as they had a low melting point than copper sheet. The workpieces were cleaned using acetone before welding to remove grease and stains that may affect the quality of welding. For the welding tool, a smooth shoulder and unthreaded conical pin were used. Table 3 shows the chemical composition of the medium carbon steel . The welding tool , which had 16mm shoulder diameter and 4mm pin base diameter, the tool was heat -treated conventionally to have a hardness of 60HRC. The tool pin shape is presented in Fig . 1a. °4 tool tilt angle was used, and the tool pin had a constant offset about 1 mm towards the Al side. FSW was conducted using a milling machine, type KAMA (X6325; 3Hp; TRPER R8; 30 KN). The spindle of milling machine was set at three different rotational speeds of 1000, 1750 and 2000 rpm, and a transverse speed of 30 mm/min. The axial force was kept constant at 7.5 KN during FSW process. The schematic diagram of the welding process is shown in Fig. 1b.

Table 1: Chemical compositions of Aluminium base metal.

Element	Al	Si	Fe	Mg	Cu	Mn
wt %	Balance	0.114	0.405	0.032	0.08	0.011

Table 2: Chemical compositions of Copper base metal.

Element	Cu	Fe	Pb	Si
wt %	Balance	0.013	0.02	0.0039

Table 3: Chemical compositions of medium carbon steel welding tool.

Element	Fe	C	Mn	P
wt %	Balance	0.44	0.79	0.012

1.2 Frictional Heat Input During FSW:

The torque required to rotate a circular welding tool relative to the surface of the workpieces under the action of an axial load is given by (Frigaard, Grong, & Midling, 2001);

$$M = \int_0^{MR} dM = \int_0^R \mu P(r) 2\pi r^2 dr = \frac{2}{3}\mu\pi \mathrm{P} r^3 \quad (1)$$

where M is the interfacial torque, μ is the friction coefficient, R is the surface radius, and p(r) is the pressure distribution across the interface (here assumed constant and equal to p).

If all the shearing work at the interface is converted into frictional heat, the average heat input per unit area and time can be represented as follow, (Frigaard *et al*., 2001);

$$q_o = \int_0^{MR} \omega dM = \omega 2\pi\mu \Pr^2 dr \quad (2)$$

where qo is the net power (in Watts) and ω is the angular velocity in (in rad/sec). The next step is to express the angular velocity in terms of the rotational speed N (in rad/sec). By substituting $\omega = 2\pi N$ into Eq. 2, the resulting heat input becomes;

$$q_o = \int_0^{R} 4\pi^2 \mu PNr^2 dr = \frac{4}{3}\pi^2 \mu PNR^3 \quad (3)$$

It was assumed that μ during FSW was almost the same value. If the contact area is Ac (R2 × π), the resulting heat flux at the stir zone is;

$$Q = \frac{q_o}{A_C} \quad (4)$$

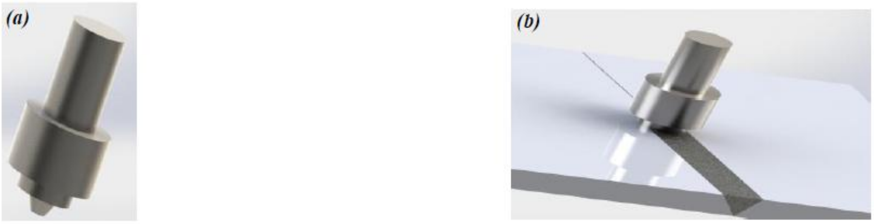

Fig. 1: (a) The welding tool geometry and (b) Schematic diagram of the FSW process.

1.3 The Laboratory Tests:

Macroscopic analysis of the welded joints at three different rotational speeds was carried out using a stereo microscope (OLYMPUS: SZ61). For the microstructural analysis, transversal sections of welds were prepared. The specifications of the cutting, grinding and polishing were performed according to the ASTM: E3 standards. All the samples were ground by rubbing with abrasive grit papers (200-1500), and then polished using 1micron diamond paste. The aluminium side was etched chemically using a solution of Keller's reagent to reveal the microstructures according to the ASTM: E407 standards. Afterward, the copper side was etched with a solution of 10gm ammonium persulfate and 100 ml distilled water. The microstructures of the specimens were observed by the optical microscope (Olympus BX41RF) and (ZEISS SUPRA 35VP) Field Emission Scanning Electron Microscopy (FESEM) in order to examine the delicate structure formed in the NZ. The welded joints were also analyzed by XRD, using a copper target to identify the phases formed in the stir zone. The instrument used in this work was D8 Advance X-ray diffractometer (Bruker Analytical X-Ray Systems). The average Vickers microhardness test was carried out on the cross-section perpendicular to the welding direction according to ASTM: E384 standards, using (FV-700E). Tensile tests were also carried out using an INSTRON (Universal Testing Machine) operated at a speed of 1 mm/min as per ASTM: E8 standards. Finally, the FESEM technique was also employed primarily to study the fractural surface of tensile specimens.

RESULTS AND DISCUSSION

2.1 Measurements of Heat Generation:

Heat is generated by the frictional process at the contact area between the tool shoulder and the workpieces. The best rotational speeds, give sufficient penetration and welds quality. The lower rotational speed result in a lower source of heat input, and a higher rotational speed result in an excessive heat input (Uday, Fauzi, Zuhailawati, & Ismail, 2011). However, the process parameter at a medium rotational speed causes good plastic deformation and sufficient penetration in the material. Three different welding rotational speeds of 1000 rpm, 1750 rpm and 2000 rpm have been calculated from Eqs. 3 and 4, in order to study the effect of rotational speeds on the heat generation. Figs. 2a and 2b show the frictional heat generation and heat flux per millimeter square area for welding rotational speeds of 1000 rpm, 1750 rpm and 2000 rpm. Based on the results, it is clear that the higher rotational speeds (2000 rpm) lead to the highest heat generation and heat flux. The frictional heat generation is reduced by about two times when the rotational speed is reduced from 2000 to 1000 rpm. This is because higher rotational speed will result in higher relative velocity of the friction; consequently, higher energy will be produced.

2.2 Results of Surface Appearance:

Fig. 3 shows the surface appearance of dissimilar FSW joints between aluminium and copper, using a low rotational speed of 1000 rpm. As seen in the Fig. 3a, semicircular metal traces are observed in the stir zone, rotational speed of 1000 rpm cannot provide enough heat to produce sound joints. Most frequently such a process leads to heating and plasticize only one side of the material and does not plasticizes the other side. However, The aluminium can be plasticized easily than copper during FSW process especially at a low rotational speed (1000 rpm) (Shukla & Shah, 2010). This is a typical feature of dissimilar FSW between aluminium and copper. Fig. 3b shows a typical unbonded joint at the root of the workpieces. This is

Journal of Applied Science and Agriculture, 10(5) Special 2015, Pages: 149-158

probably due to facing difficulties of supplying sufficient heat to the root flat surfaces. Moreover, it might be due to unexpected misalignment of the workpieces during welding process, or poor interaction between the pin and the welded sheets (Bahemmat, Rahbari, Haghpanahi, & Besharati, 2008). The pin plunging depth is a very critical factor and difficult to be controlled. The depth of sinking must be constant along the welding process. However, it is very hard to achieve, and also preparation of the surface before welding is critical and must draw a lot of attention (Meran, 2006). The dissimilar joining of aluminium and copper gives a very low strength; most of the samples were fractured during the sample cutting.

Fig. 4 shows the welding profile of dissimilar FSW joints of aluminium and copper, using a rotational speed of 1750 rpm. Fig. 4a shows no defects at the top side of the joint, it can be seen only a small amount of welding flash at the copper side. In addition, the welding zone at the top side is completely covered with aluminium metal. This is so because at the same processing tempeature, aluminium has a better plastic flowability than copper due to its lower melting point. Fig. 4b shows a completely filled groove with no defects, rotational speed of 1750 rpm can provide sufficient heat input and pin plunge depth involvs greater engagement.

At a high rotational speed of 2000 rpm, the surface morphology of the stir zone became rough as opposed to that conducted at 1750 rpm. Fig. 5a shows particles of copper spread with aluminum which indicates excessive mixing of the material during this welding process. The high temperatures associated with a strong stirring action of the pin tool result in the formation of intermetallic compounds (Al2Cu and Al4Cu9). Fig. 5b shows a poor welded region at the bottom surfaces due to excessive heat generation (Abdollah-Zadeh, Saeid, & Sazgari, 2008).

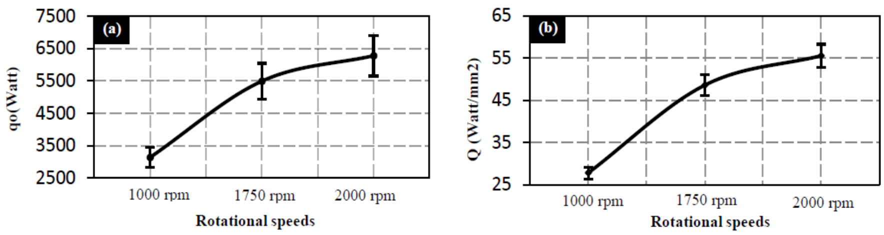

Fig. 2: The effect of rotational speeds on (a) the frictional heat generation and (b) the frictional heat flux.

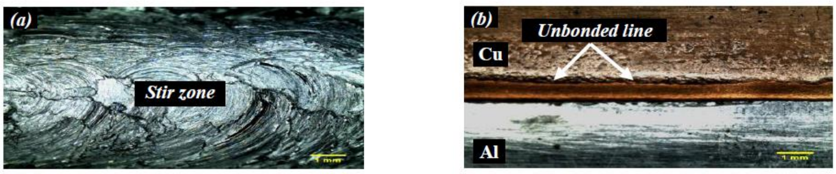

Fig. 3: Optical macrograph of dissimilar aluminium and copper joint, FSW at a rotational speed of 1000; (a) Top view and (b) Bottom view.

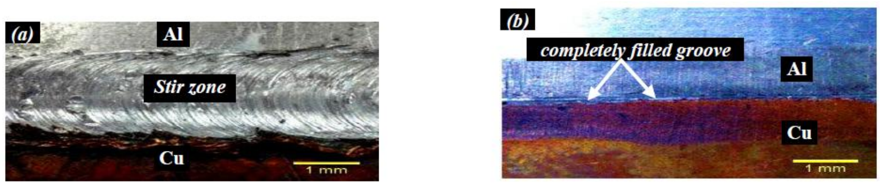

Fig. 4: Optical macrograph of dissimilar aluminium and copper joint, FSW at a rotational speed of 1750; (a) Top view and (b) Bottom view.

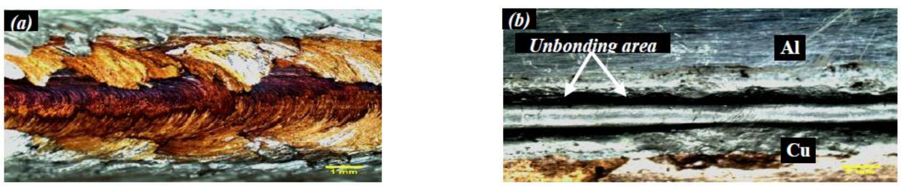

Fig. 5: Optical macrograph of dissimilar aluminium and copper joint, FSW at a rotational speed of 2000; (a) Top view and (b) Bottom view.

2.3 Microstructures Analysis:

Fig. 6 shows the schematic diagram for the different welding zones; the NZ in the centre of the weld line where the pin has passed. TMAZ is immediately adjacent to NZ. HAZ is located between TMAZ and the unaffected BM which experiences a

Journal of Applied Science and Agriculture, 10(5) Special 2015, Pages: 149-158

thermal cycle. BM is a remote material from the weld center, and from the experimental perspective, it has a thermal cycle from the weld which is not affected by the heat in terms of microstructure or mechanical properties (Jata & Semiatin, 2000; G. Liu, Murr, Niou, McClure, & Vega, 1997; Salem, Reynolds, & Lyons, 2002). There is a remarkable differences in the internal structures of the NZ and the TMAZ; whereas the NZ is composed of fine-equiaxed recrystallization grains, the TMAZ is composed of coarse-bent recovered grains where no recrystallization is observed. Evidence from previous studies, suggest that the recrystallized grains in the NZ are due to mechanical action of the pin tool that generates a continuous dynamic recrystallization process (H. Liu, Fujii, Maeda, & Nogi, 2003).

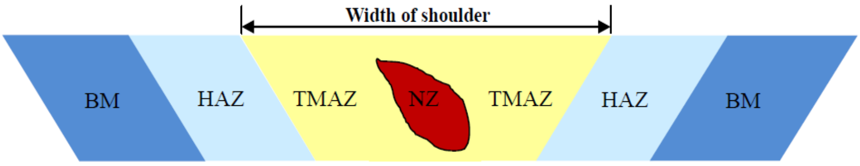

Fig. 6: Welding zones after FSW process.

Fig. 7a shows the aluminium BM of an elongated grain structure while Fig. 7b shows the microstructure of copper BM, having a mixture of fine and coarse irregular grains. The optical micrograph of the joints produced at 1750 rpm (Fig. 8a) shows the different regions between aluminium and copper joint. TMAZ can be clearly seen at aluminium side because aluminium has a lower hardness and a melting point than copper. However, at the same temperature and force acting on both metals, copper experiences a lesser effect than aluminium. The grains of HAZ are coarser than TMAZ due to contrasting effects of stirring and thermal exposure. Finer grains can be observed in Fig. 8b, which indicates that this region is NZ, the dissimilar metals welded at a rotational speed of 2000 rpm. Near the interface, a detached copper layer can be seen clearly surrounded with aluminium. It is also noted that aluminium has penetrated into the lamellar structure on the copper side, which leading to form a new interface between the welded joint. A darker region in the interface indicates that aluminum is rich; while a brighter region indicates that copper is rich. The copper side shows a severe plastic deformation due to the effects of stirring action and frictional heat, which that indicated a damaged of surface layer of the copper near the welded interface. The effect of increasing rotational speed over the friction-welding joint resulted in an increase in the temperature gradient as a result of increased deformation at the welding interface. High temperatures with strong stir action of welding tool result in the formation of intermetallic compounds which decreases the tensile strength of the welded joint and increases the microhardness (Shukla & Shah, 2010). As the rotational speed increases, the time to reduce the maximum temperature at the interface decreases and consequently, the cooling gradient becomes steep due to the rapid heat adsorption by the adjacent region. This led to change the microstructure in the HAZ and caused an increase in the viscous forces with maximum transfer of the subjected matter out of the interface.

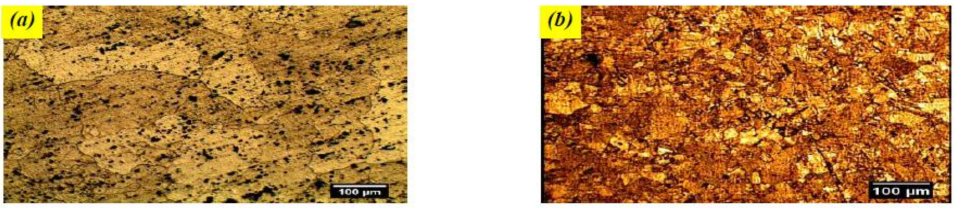

Fig. 7: Microstructures of the base materials, (a) Aluminium base metal and (b) Copper base metal.

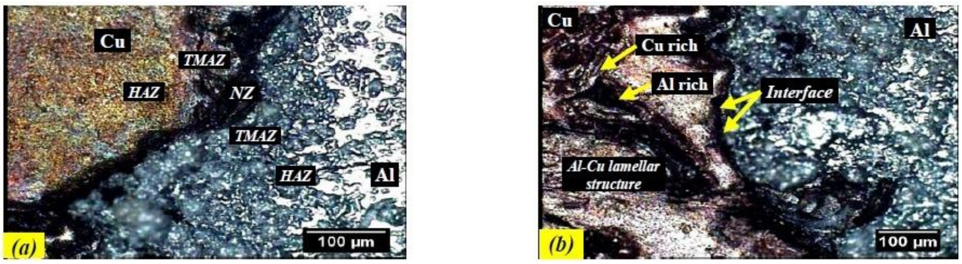

Fig. 8: Microstructural analysis of dissimilar aluminium and copper joints friction stir welded at; (a) 1750 rpm and (b) 2000 rpm.

Table 4: The grain sizes of different welding zones of Al and Cu conducted at three rotational speeds.

Rotational speeds	Grain size at Al side (µm)			Grain size at Cu side (µm)			Al-base metal (µm)	Cu-base metal (µm)
	NZ	TMAZ	HAZ	NZ	TMAZ	HAZ		
1000 rpm	~9.3	~11.8	~156	~2	~5.7	~68.2	~172	~70
1750 rpm	~11.8	~13.9	~162	~5.5	~9.4	~76.1	~172	~70
2000 rpm	~13.1	~16.5	~178	~8.1	~11.8	~89.6	~172	~70

Fig. 9a shows the FESEM of FSW aluminium and copper sample at a rotational welding speed of 1000 rpm. As shown in the figure, the interface between Al-Cu consists of a bonded and unbonded joint, which means that this joint is relatively weak. A lower rotational speed will result in a lower relative velocity of the friction; consequently, lower energy will be produced. According to the EDX analysis, Fig. 10a shows the analysis of the location area at the interface which consists of aluminium and copper. EDX analysis reveals that the ratio of aluminium to copper is about 3.9. On the contrary, only aluminium and copper are observed in the joint FSW at 1000 rpm. This fact is in fully agreement with data reported for dissimilar FSW of aluminium and copper (LI, ZHANG, QIU, & ZHANG, 2012). Fig. 9b shows the interface of FSW dissimilar aluminium and copper sample at a welding rotational speed of 1750 rpm. As clearly seen in the figure, the interface consists of uniform distribution of sluminium and copper particles. Probably, this is due to sufficient frictional heat generated. This interlaced structure formed by aluminium and copper indicates that the dissimilar sheets are bonded together firmly in this region. The EDX analysis in Figure. 10b shows that the bonded area also consists of aluminium and copper. However, the wt% of aluminium to copper is about 1.9. Some cracks can be observed in Fig. 9c, which indicates that a severe plastic deformation has taken place during FSW process at a higher rotational speed of 2000 rpm. However, some intermetallic compounds exist in the interface between aluminium and copper due to the excessive frictional heat input.

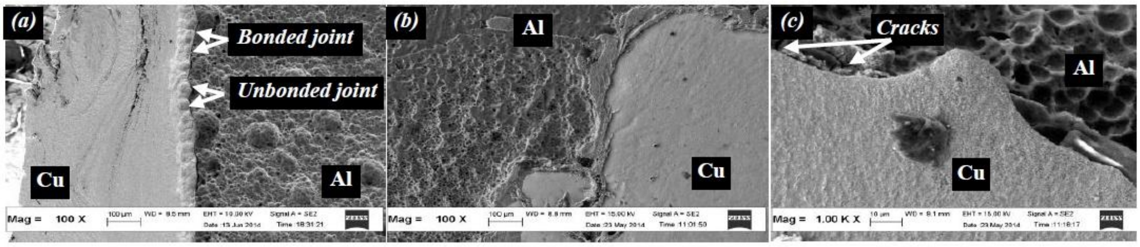

Fig. 9: FESEM analysis of dissimilar aluminium and copper friction stir welded at; (a) 1000 rpm (c) 1750 rpm and (d) 2000 rpm.

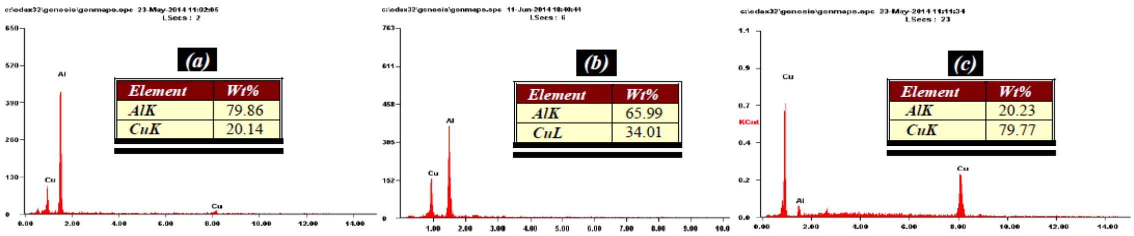

Fig. 10: EDX analysis of dissimilar aluminium and copper joints friction stir welded at the diferent rotational speeds, (a) 1000 rpm, (b) 1750 rpm and (c) 2000 rpm.

2.4 X-Ray Diffraction (XRD) Analysis:

XRD analysis was also examined in order to identify the composition of phases in FSW region, using a copper target. The results of XRD pattern are shown in Fig. 11. The relevant parameters corresponding to the diffraction peaks in the diagram have been computed using X' Pert High Score Plus software. The analysis indicates that aluminium and copper as a cubic structure. The figure shows the XRD analysis for dissimilar FSW aluminium and copper in the stir zone at the three different rotational speeds of 1000, 1750 and 2000 rpm. As shown in Fig. 11a, intermetallic compounds (Al2Cu and Al4Cu9) are formed in the NZ at a rotational speed of 2000 rpm. This means that a chemical reaction has occurred between the aluminium and copper during welding process. Hard brittle intermetallic compounds between dissimilar joint of aluminum and copper are formed through the liquid state reaction which is resulted from the high rotational speed and phase transformation due to excessive heat generation (Meran, 2006). Figs. 11b and c, shows only aluminium and copper formed in the dissimilar FSW joints at 1750 and 1000 rpm, and no aluminium-copper intermetallic compounds can be seen. This indicates that neither chemical reaction between aluminium and copper and nor phase transformation has occurred during the dissimilar FSW process, this findin is in consistence with the results by (LI *et al*., 2012). The XRD data in Table 5 shows changes occurred in metal density, crystallite size and lattice parameters at the joints FSW with three different rotational speeds. These computed results were compared with the relevant parameters of the base materials. The XRD analysis of aluminium and copper which matched with the reference code 98-009-1623and 98-000-6366, respectively. This observation of transient microstructure is important in understanding the complicated friction welding process which includes the plastic deformation and dynamic recrystallization at changeable rotational speeds.

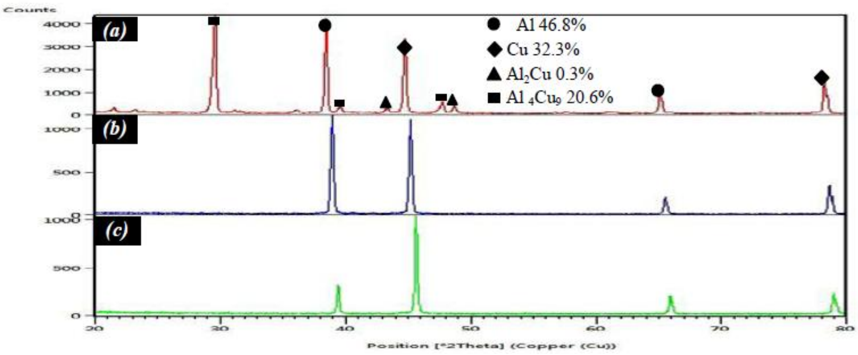

Fig. 11: XRD analysis of the welded joints FSW at a: (a) 2000 rpm, (b) 1750 rpm and (c) 1000 rpm.

Table 5: XRD results of commercially available pure Al and Cu base materials and the joints FSW at different rotational speeds near the interface.

Relevant parameters	Al base metal	Cu base metal	Welded joints at different rotational speeds (rpm)		
			1000	1750	2000
Density (calculated) (gm/cm³)	2.6979	8.8898	8.6280	6.4605	5.1136
Crystallite size (nm)	68.77	53.65	48.72	68.72	73.49
Lattice parameters (a, b, c) °A	4.0498	3.6209	3.6171	8.8742	12.137

2.5 Microhardness and Tensile Measurements:

Fig. 12a demonstrates the microhardness profiles of the dissimilar FSW aluminium and copper from the center line of the welded joints at the three different rotational speeds. The figure shows a higher microhardness at the NZ. The microhardness is slightly higher than those of the base metals, mainly due to the formation of hard brittle intermetallic compounds (Al2Cu and Al4Cu9) during FSW process, especially at the rotational speed of 2000 rpm. A higher tool rotational speed results in a higher heat input and a slower cooling rate leads to the formation of hard brittle intermetallic compounds in the NZ. On the other hand, a lower heat input condition due to a lower rotational speed (1000 rpm) results in a lack of stirring action and causes the formation of defects, without forming intermetallic compounds (Elangovan & Balasubramanian, 2007). Microhardness values of the FSW joints at a rotation speed of 1000 and 1750 rpm which were much higher than that of the base metals. This may be due to the existence of large copper particles and layers; these copper layers have a high microhardness value. This is probably developed during FSW process, and produces a high dislocation density; that is why a high microhardness value can be observed at the rotation speeds of 1000 and 1750 rpm. In addition, the microhardness in the NZ increases slightly with the decrease in the grain size through the following relationship (Hirata *et al*., 2007);

$$HV = H_0 + KHd^{-1/2} \quad (5)$$

where HV is the hardness, Ho a n d kH are the appropriate constants associated with the hardness measurements. It was concluded that the microhardness of the NZ increases with the decrease in friction heat flow; whereas the grain size in the NZ decreases when the friction heat flow decreases (Hirata *et al*., 2007).

Fig. 12b shows the comparison of tensile strengths between the welded joints and the base materials at the three different rotational speeds. At the rotational speed of 1750 rpm, the tensile strength is higher than that of 1000 and 2000 rpm. The tensile strength of the joint FSW at the rotational speed of 2000 rpm shows a lower value because this joint is only created mainly by the bonds of adhesion which results in a low tensile strength. The low tensile strength is mainly due to the formation of intermetallic compounds (Al2Cu and Al4Cu9) and cracks. Moreover, all the samples are fractured in the aluminium side near the NZ, because during FSW the materials in the NZ are exposed to severe plastic deformation which causes a very fine grain structure in comparison to that of TMAZ, and consequently it leads to a higher value of strength. The dissimilar fractural location between aluminium and copper were also reported by XUE *et al*. (Xue, Ni, Wang, Xiao, & Ma, 2011). Besides, the tensile strength of aluminium base metal is lesser than the copper base metal; therefore, most of the specimens are fractured from aluminium side (Shukla & Shah, 2010). Table 6 lists the tensile properties (yield elongation and break elongation) of the dissimilar aluminium and copper FSW joints, which illustrate that the best elongation and break elongation of the joint that is FSW at 1750 rpm are 4.26 % and 9.3 %.

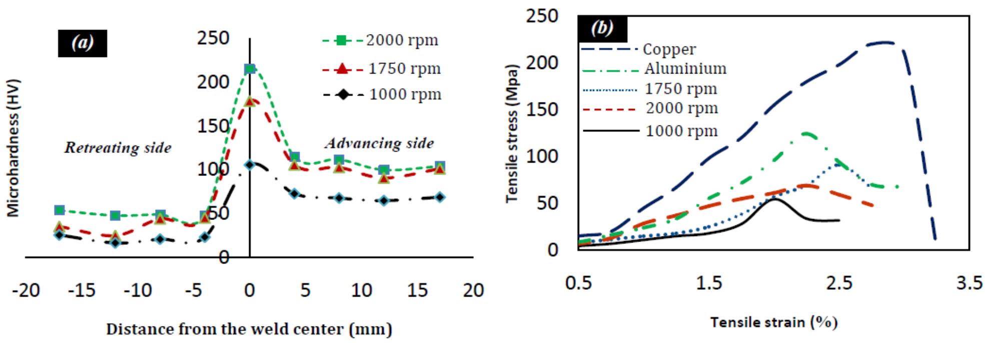

Fig. 12: (a)The average transverse microhardness across the welded joints and (b) Tensile strain-stress curves of FSW dissimilar aluminium and copper joints compared to the base materials.

Table 6: Tensile properties of Al-Cu FSW joints.

Rotational speeds (rpm)	Yield elongation (%)	Break elongation (%)
1000	2.10	5.1
1750	4.26	9.3
2000	1.56	1.9

2.6 Fractography:

To obtain a better understanding of the failure micro mechanism of the FSW zone, a fractographic examination was carried out on the fractural surfaces of tensile test specimens using FESEM. Fig. 13 illustrates the FESEM images of the tensile fractural surfaces. Fig. 13a shows the tensile fracture surface FSW at 1000 rpm. The fractural features indicate that the failure area is at the aluminium side beside the NZ. Voids could also be seen at some fractural regions at the aluminium side, which suggest that this side is relatively weak. Ductile fracture mode is found at a joint fabricated with a rotational speed of 1750 rpm (Fig. 13b). Brittle fractures and cracks are observed on the fractural features FSW at a rotational speed of 2000 rpm (Fig. 13c). The figure shows an uneven surface and complex microstructures at the NZ. This fractural surface features showed that all parts of the fractural surface exhibited a typical brittle fractural mode with some detected of copper particles in some parts of the aluminum side. Therefore, the fractural mode of the dissimilar joints can be defined as a ductile and brittle fracture.

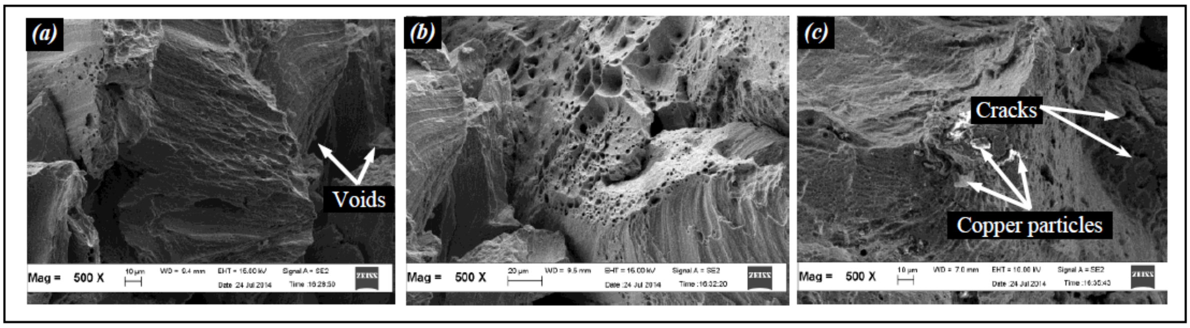

Fig. 13: FESEM images showing a tensile fracture surface mode of FSW dissimilar aluminium-copper joints; (a) 1000 rpm, (b) 1750 rpm and (c) 2000 rpm.

3. Conclusions:

Commercially available pure aluminium and copper have been joined successfully by FSW conditions. There is a range of rotational speed or heat input in which the specimen can be joined together successfully, especially at 1750 rpm. Several forms of brittle intermetallic compounds were found in the joint FSW at a high rotational speed of 2000 rpm. These compounds mainly consist of Al2Cu and Al4Cu9. The microhardness of the NZ showed superior values than that of base materials indicating multiple contradiction effects of work hardening, brittle intermetallic compounds and grain refinement (recrystallization). Regarding tensile strength results, a lower strength was obtained at FSW with a high rotational speed of 2000 rpm due to the intermetallic phase formation. The weakest part of welded joints is aluminium side near the NZ. The fractural mode of the dissimilar joints can be defined as a ductile and brittle fracture. The fractural mode has a tendency to change from ductile to brittle mode, with an increasing in the heat input or rotational speeds.

ACKNOWLEDGEMENTS

This work was supported under the grant No. 9001-00338 of the Universiti Malaysia Perlis (UniMAP). The authors gratefully acknowledge the outstanding support provided by the staff in the Materials Engineering School, Universiti Malaysia Perlis (UniMAP), UTM Centre for Low Carbon Transport, in cooperation with Imperial College London, Transportation Research Alliance, Universiti Teknologi Malaysia (UTM) and the School of Materials Engineering and Mineral Resources in Universiti Sains Malaysia (USM).

REFERENCES

Abdollah-Zadeh, A., T. Saeid, B. Sazgari, 2008. Microstructural and mechanical properties of friction stir welded aluminum/copper lap joints. *Journal of Alloys and Compounds, 460*(1): 535-538.

Bahemmat, P., A. Rahbari, M. Haghpanahi, M. Besharati, 2008. Experimental study on the effect of rotational speed and tool pin profile on aa2024 aluminium friction stir welded butt joints. *Proceedings of ECTC 2008, October 3-4, 2008, Miami, Florida, USA., p 1.1, 1*.

Elangovan, K., V. Balasubramanian, 2007. Influences of pin profile and rotational speed of the tool on the formation of friction stir processing zone in AA2219 aluminium alloy. *Materials Science and Engineering: A, 459*(1): 7-18.

Frigaard, Ø., Ø. Grong, O. Midling, 2001. A process model for friction stir welding of age hardening aluminum alloys. *Metallurgical and materials transactions A, 32*(5): 1189-1200.

Galvao, I., J.C. Oliveira, A. Loureiro, D.M. Rodrigues, 2011. Formation and distribution of brittle structures in friction stir welding of aluminium and copper: influence of process parameters. *Science and Technology of Welding and Joining, 16*(8): 681-689.

Hirata, T., T. Oguri, H. Hagino, T. Tanaka, S.W. Chung, Y. Takigawa, K. Higashi, 2007. Influence of friction stir welding parameters on grain size and formability in 5083 aluminum alloy. *Materials Science and Engineering: A, 456*(1): 344-349.

Jata, K., S. Semiatin, 2000. Continuous dynamic recrystallization during friction stir welding of high strength aluminum alloys: DTIC Document.

Kwon, Y.J., S.B. Shim, D.H. Park, 2009. Friction stir welding of 5052 aluminum alloy plates. *Transactions of Nonferrous Metals Society of China, 19:* s23-s27.

Li, X.W., D.T. Zhang, C. Qiu, W. Zhang, 2012. Microstructure and mechanical properties of dissimilar pure copper/1350 aluminum alloy butt joints by friction stir welding. *Transactions of Nonferrous Metals Society of China, 22*(6): 1298-1306.

Liu, G., L. Murr, C. Niou, J. McClure, F. Vega, 1997. Microstructural aspects of the friction-stir welding of 6061-T6 aluminum. *Scripta materialia, 37*(3): 355-361.

Liu, H., H. Fujii, M. Maeda, K. Nogi, 2003. Tensile properties and fracture locations of friction-stir-welded joints of 2017-T351 aluminum alloy. *Journal of Materials Processing Technology, 142*(3): 692-696.

Liu, P., Q. Shi, W. Wang, X. Wang, Z. Zhang, 2008. Microstructure and XRD analysis of FSW joints for copper T2/aluminium 5A06 dissimilar materials. *Materials letters, 62*(25): 4106-4108.

Meran, C., 2006. The joint properties of brass plates by friction stir welding. *Materials & design, 27*(9): 719-726.

Mishra, R.S., Z. Ma, 2005. Friction stir welding and processing. *Materials Science and Engineering: R: Reports, 50*(1): 1-78.

Nandan, R., T. DebRoy, H. Bhadeshia, 2008. Recent advances in friction-stir welding–process, weldment structure and properties. *Progress in Materials Science, 53*(6): 980-1023.

Ouyang, J., E. Yarrapareddy, R. Kovacevic, 2006. Microstructural evolution in the friction stir welded 6061 aluminum alloy (T6-temper condition) to copper. *Journal of Materials Processing Technology, 172*(1): 110-122.

Salem, H.G., A.P. Reynolds, J.S. Lyons, 2002. Microstructure and retention of superplasticity of friction stir welded superplastic 2095 sheet. *Scripta materialia, 46*(5): 337-342.

Shukla, R.K., P.K. Shah, 2010. Comparative study of friction stir welding and tungsten inert gas welding process. *Indian Journal of Science and Technology, 3*(6): 667-671.

Uday, M., A. Fauzi, H. Zuhailawati, A. Ismail, 2011. Effect of welding speed on mechanical strength of friction welded joint of YSZ–alumina composite and 6061 aluminum alloy. *Materials Science and Engineering: A, 528*(13): 4753-4760.

Vural, M., A. Ogur, G. Cam, C. Ozarpa, 2007. On the friction stir welding of aluminium alloys EN AW 2024-0 and EN AW 5754-H22. *Archives of Materials Science and Engineering, 28*(1): 49-54.

Journal of Applied Science and Agriculture, 10(5) Special 2015, Pages: 149-158

Weigl, M., F. Albert, M. Schmidt, 2011. Enhancing the ductility of laser-welded copper-aluminum connections by using adapted filler materials. *Physics Procedia, 12:* 332-338.

Xue, P., D. Ni, D. Wang, B. Xiao, Z. Ma, 2011. Effect of friction stir welding parameters on the microstructure and mechanical properties of the dissimilar Al–Cu joints. *Materials Science and Engineering: A, 528*(13): 4683-4689.